Supplemental Materials

Molecular Biology of the Cell

Ajjaji et al.

Supplementary Figure 1 (related to Figure 1)

(A) Endogenous Plin expression was evaluated by western blot in Huh7, 3T3 D12 adipocytes and Hela cells. Calnexin was used as loading control.

(B) The left hand panel shows the localization (LD (lipid droplet)/cytosol) of the GFP-tagged Plins(1-3)-**C** in Huh7 cells. Scale bar, 10 μm. Zoomed in views of the insets are shown on the right. The fluorescence profiles of lines drawn in the insets are shown on the far right (LD in red, Protein in green). Localization of proteins at the LD surface gives two clear green peaks around the red LD signal. The far right-hand panel shows the % of LDs in cells having the protein at their surface. 15–20 cells were combined for analysis, corresponding to a total number of LDs of ~1500.

(C) Representative images of the relative localization (Nucleus/Cytosol) of GFP-tagged fragments of the Plin(1-3)-**N** (right panel) and Plin(1-3)-**C** (left panel). Scale bar, 10 μm.

(D) Representative image of the GFP-FL Plin1 and mCherry-Sec61 beta colocalization in Huh7 cells. The inset squares indicate colocalization of the two proteins; colocalization was analysed by Fiji, and the Pearson's coefficient reveals a high degree of colocalization (F). Data are expressed as means ± SEM. Scale bar, 10 μm.

(E) Representative image of the Plin1-**C** GFP-tagged and mCherry-Sec61 beta colocalization in Huh7 cells. The inset squares indicate colocalization of the two proteins; colocalization was analysed by Fiji, and the Pearson's coefficient reveals a high degree of colocalization (F). Data are expressed as means ± SEM. Scale bar, 10 μm.

(G) HeLa cells were transfected with GFP-tagged full-length (FL), Plin-**N** and Plin-**C** perilipin constructs. Four hours post transfection, cells were loaded with 400 μM oleic acid and BODIPY 558/568 C_{12} for 20 h prior to fixing. Cells were imaged using confocal microscopy. Scale bars, 10 μm. Images are representative of 2 – 3 independent experiments.

Supplementary Figure 2 (related to Figure 1 and Figure 2)

A) Carboxy-terminal domain of Plin3 (Hickenbottom et al., 2004) (PDB ID 1szi) consisting of a 4HB (aa 244-412) zipped together by 4 strands of β-sheet (position in

the alignment below). Top: topology of the secondary structure elements; bottom left: 3D structure; bottom right: schematic illustration of the 4HB structure with helices represented as cylinders and β-sheets as arrows. The name "4HB" is used for this domain throughout the paper. Homology indicates that the structure of Plins 2, 4 and 5 are very similar in this region while Plin1 does not contain the stabilising β-sheet (Hickenbottom et al., 2004; Rowe et al., 2016).

B) Comparison of the sequences known to form β-sheets in mouse Plin3 (1szi) with corresponding segments in human Plins. The intensity of the blue background indicates the amino acid identity, the bars represent the strands of β-sheet and the arrow depicts the position of the beginning of the Plin1 unique extra exon with evolutionary unrelated sequence.

(C) FRAP analysis of the Plin1-**C** and FL Plin1 co-expressed in Huh7 cells. The inset squares indicate the bleached region in the second panel from the left and then subsequent panels show this region immediately after bleaching and then at the indicated times thereafter. Scale bar, 10 µm. The experiment was repeated twice and the normalized fluorescence intensity evolution of the bleached LD cluster is shown for the displayed representative sequence.

(D) FRAP analysis of the Plin1-**C** and FL Plin2 co-expressed in Huh7 cells. The insert squares indicate the bleached region in the second panel from the left and then subsequent panels show this region immediately after bleaching and then at the indicated times thereafter. Scale bar, 10 µm. The experiment was repeated three times and the normalized fluorescence intensity evolution of the bleached LD cluster is shown for the displayed representative sequence.

(E) GFP-FL Plin1 co-expression and LD colocalization with mCherry-FL Plin2 in Huh7 cells. The insert squares indicate the colocalization region of corresponding proteins to the LD surface. The relative bound fraction level is reported on the right panel and indicates that GFP-FL Plin1 displaces mCherry-FL Plin2 from the LD surface. A similar displacement is observed in Figure 2A but with switched tags. GFP/mCherry does not affect the behaviour of the constructs. Each experimental dot corresponds to an average of the signal on 10 to 20 LDs. Scale bar, 10 µm.

(F) Expression of endogenous Plin2,3 was evaluated by western blot in Huh7 cells transfected with eGFP-Plin1 (left panel) and eGFP-Plin2 (right panel). β-actin was used as loading control.

(G) Western blot analysis using antibodies to endogenous Plin3 in Huh7 cells transfected with eGFP-Plin3 and eGFP- Plin3-β. GAPDH was used as loading control.

(H) Images of eGFP-Plin3-β and eGFP-Plin3 signal localizing to LDs when expressed alone in Huh7 cells. The insert squares indicate localization region of corresponding protein to the LD surface. Under the same settings, eGFP-Plin3-β always displayed more important signals around LDs than eGFP-Plin3. Scale bar, 10 µm.

(I) The relative bound fraction level of eGFP-Plin3-β co-expression with mCherry-FL Plin3 (shown in figure 2I) is reported and indicates that mCherry FL Plin3 is readily displaced from LDs when coexpressed with eGFP-Plin3-β. Each experimental dot corresponds to an average of the signal on 10 to 20 LDs.

Supplementary Figure 3 (related to Figure 2)

(A) Representative images of GFP-FL Plin1 and mCherry-FL Plin2 when co-expressed and analysed with FRAP in Huh7 cells. FRAP image sequences and quantification are shown. The experiments were replicated three times. Scale bar, 10 µm.

(B) Signal recovery over time of Plin1 FL and Plin1-**N** and (C) of FL Plin1 and Plin1-**C** when co-expressed. The experiments were replicated three times.

(D) Histograms of characteristic recovery time for FL Plin1, vs. FL Plin2 and vs. Plin1 fragments deduced from (A, B, C).

(E) mCherry-FL Plin1 co-expression and colocalization with GFP-tagged FL Plin2. Plin1 and Plin2 are enriched on different LD subpopulations. Scale bar, 10 µm.

(F) mCherry-FL Plin3 co-expression and colocalization with GFP-tagged versions of FL Plin2 and Plin1 fragments. Representative images are shown. This experiment was repeated at least two times. Scale bar 10 µm. The fall off level of the experiments are described in the lower panel. Each experimental dot corresponds to an average of the signal on 10 to 20 LDs.

(G) Critical concentrations for FL Plin3 displacement by Plin2 and Plin1 fragments are reported (from (F)), ns. not significant. Results are presented as box-and-whisker plots of the critical concentration. The central box represents the interquartile ranges (25th to 75th percentile), the middle line represents the median and the horizontal lines represent the minimum and the maximum value of observation range. Values are expressed as median ± IR.

(H) mCherry-Plin1-**N** co-expression with GFP-tagged versions of the other fragments of Plins1-3 in Huh7 cells. The insert squares are zoomed in images of LDs. Scale bar, 10 µm. The bound fraction level is reported in the right panel and indicates the amount of the mCherry-Plin1-**N** (the reference protein) required to displace the 'competing' protein from the LD surface. Scale bar, 10 µm.

(I) mCherry-Plin2-**C** co-expression and colocalization with the GFP-Plin3-**N** or GFP-FL Plin3; and GFP-Plin2-**C** co-expression and colocalization with the mCherry-Plin1-**N**. Representative images are shown and the experiment was repeated twice. Scale bar 10 µm. The 4HB region of Plin2 is readily displaced from LDs when coexpressed with the other proteins that localise to LDs.

Supplementary Figure 4 (related to Figure 3)

(A-B) GFP/mCherry do not affect the behaviour of proteins. GFP-FL Plin1 and mCherry-Plin1-**N** shows similar latteral diffusion (A) and fall off (B) as with the switched tags, seen respectively in Figure 3E and Figure 3F with mCherry-FL Plin1 and GFP-Plin1-**N**. Experiment was repeated three times. For (B), Fluorescence intensity profile during shrinkage is plotted against the droplet compression factor (right panels). In the far-right panel, the mean ± SD surface/lumen signal during compression is reported. Scale bar, 30 µm.

(C-D) FL Plin1 and Plin1-**C** have conserved relative diffusion rates regardless of their GFP or mCherry tags. Experiment was repeated three times. Representative image sequences are shown. Scale bar, 30 µm.

(E) Lateral recovery of mCherry-FL Plin2 against GFP-Plin-**C** at the buffer-in-oil interface is reported. Representative images are shown. Scale bar, 30 µm. Mean fluorescence recovery ± SD on the bleached droplet surface area over time is shown (right). The experiments were repeated twice.

(F) The level of mCherry-FL Plin2 and GFP-Plin1-**C** upon interface shrinkage is shown. Scale bar, 30 μm. Fluorescence intensity profile during shrinkage is plotted against the droplet compression factor (right panels). In the far-right panel, the mean ± SD surface/lumen signal during compression is reported. The experiment was reproduced 3 times.

Supplementary Figure 5 (related to Figure 4)

(A) (left panel) Schematic illustration of the interaction of peptides with a naked triolein-buffer interface. (right panel) The effect of Plin1 (amino acids 93-192) wild type (WT, black line, upper panel) and mutant (L143D, red line, lower panel) peptides on the interfacial tension of a triolein/water (TO/W) interface. The same initial data is shown in Figure 4B, but here the data for several subsequent compression/ re-expansion cycles is included.

(B) (left panel) Schematic illustration of the oil droplet with both phospholipid (POPC) and peptide added. (right panel) The effect of WT (black line, upper panel) and L143D mutant (red line, lower panel) peptide addition to a TO/W/POPC interface on surface tension before and after several surface compressions. Here we also include data following 'washout' of the residual peptide in the buffer. In this case, each compression is associated with net loss of peptide so the equilibrium surface tension rises progressively back towards the initial surface tension following addition of POPC alone.

(C) Competition for the POPC/TO/W interface between Plin1 93-192 WT and mutant L143D. Initial addition of phospholipid (+POPC arrow) to the buffer slowly reduced surface tension to ~ 26 mN/m (γ_{eq}). POPC in the aqueous phase was removed by washout. Following addition of 10 μg of mutant L143D (+L143D arrow) to the buffer, surface tension promptly fell to ~17.3 mN/m(γeq). The area was then reduced by ~30% causing the tension to fall rapidly before returning to a lower surface tension of ~15-16 mN/m. The area was then re-expanded and tension spiked before falling back to γeq. An equivalent amount of Plin1 WT peptide was then also injected (+WT arrow) and surface tension slowly fell to a new γ_{eq}. of ~14.7 mN/m indicating that WT displaced the mutant peptide. The surface tension profile following a repeat compression and re-expansion was somewhat different to that recorded during a

similar compression in the presence of mutant peptide alone, insofar as there was a 'shoulder' (similar to that seen on the TO/W interface (see Figure 4E)) in the recovery period – we interpret this as reflecting initial rapid re-association of both mutant and WT peptide with the interface but then over time, the mutant is entirely displaced by the WT peptide.

(D,E) The maximum pressure the peptide can withstand without being ejected from the interface is referred to as Π_{max}. Data from a number of rapid compression experiments plotting the maximum Π (Π_0) obtained for a given compression is plotted against the change in ($\Delta\gamma$) after compression. The extrapolations to $\Delta\gamma = 0$ give Π_{max} for each peptide on the two interfaces. (D) The Π_{max} for the WT (black) and L143D mutant (red) peptide is shown for the TO/W interfaces. Π_{max} was consistently higher for the WT than for the mutant peptide. (E) Similarly to the Plin1 WT peptide (Figure 4G), the Π_{max} for the L143D mutant was consistently higher in the presence of POPC (green circles) than in its absence (red). Values for Π_{max} are summarized in Figure 4H.

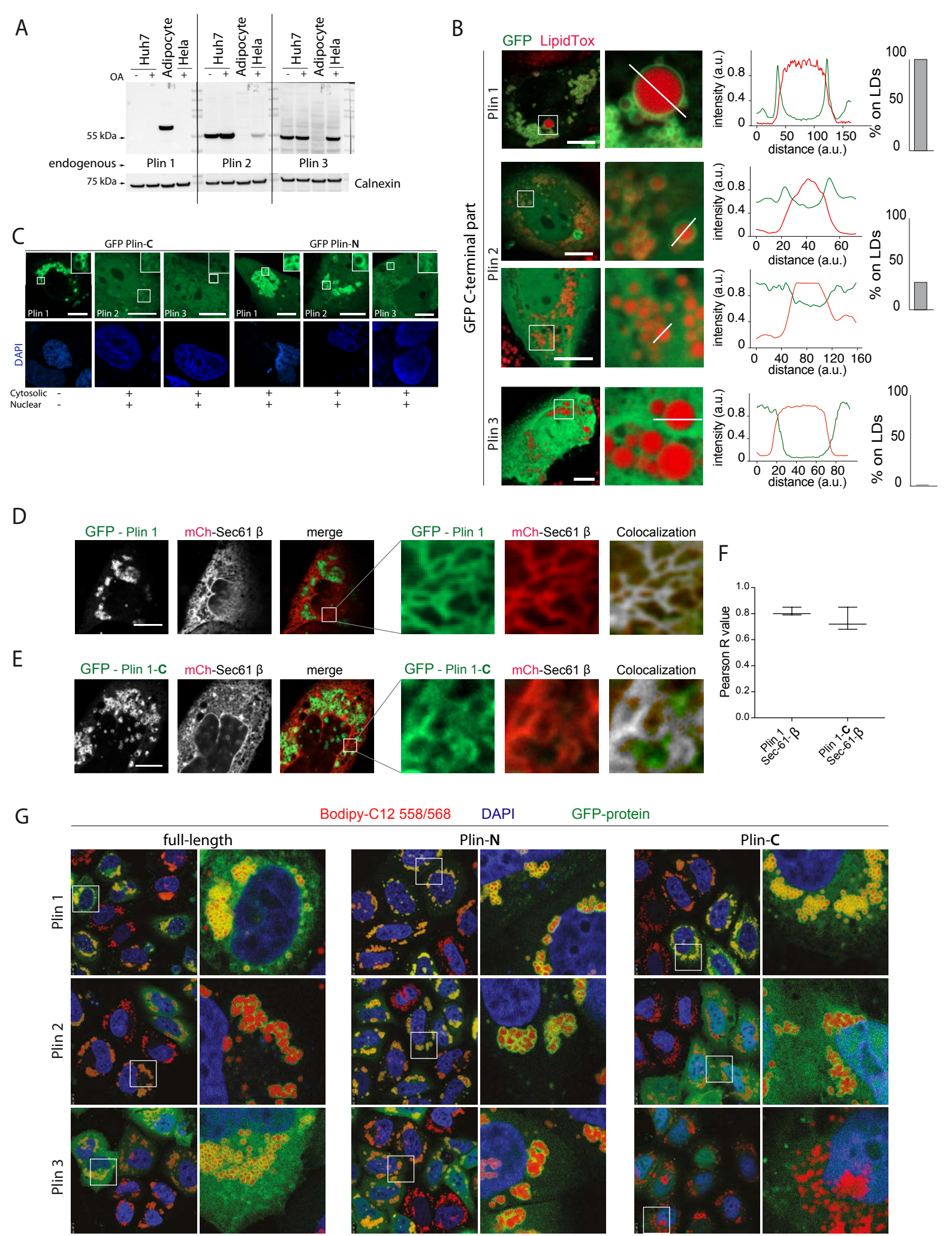
A
Huh7
Adipocyte
Hela
OA
55 kDa
endogenous
Plin 1
Plin 2
Plin 3
75 kDa
Calnexin
B
GFP LipidTox
GFP C-terminal part
Plin 1
Plin 2
Plin 3
intensity (a.u.)
distance (a.u.)
% on LDs
C
GFP Plin-C
GFP Plin-N
DAPI
Cytosolic
Nuclear
D
GFP - Plin 1
mCh-Sec61 β
merge
Colocalization
E
GFP - Plin 1-C
F
Pearson R value
Plin 1
Sec-61-β
Plin 1-C
G
Bodipy-C12 558/568
DAPI
GFP-protein
full-length
Plin-N
Plin-C

Figure 1S

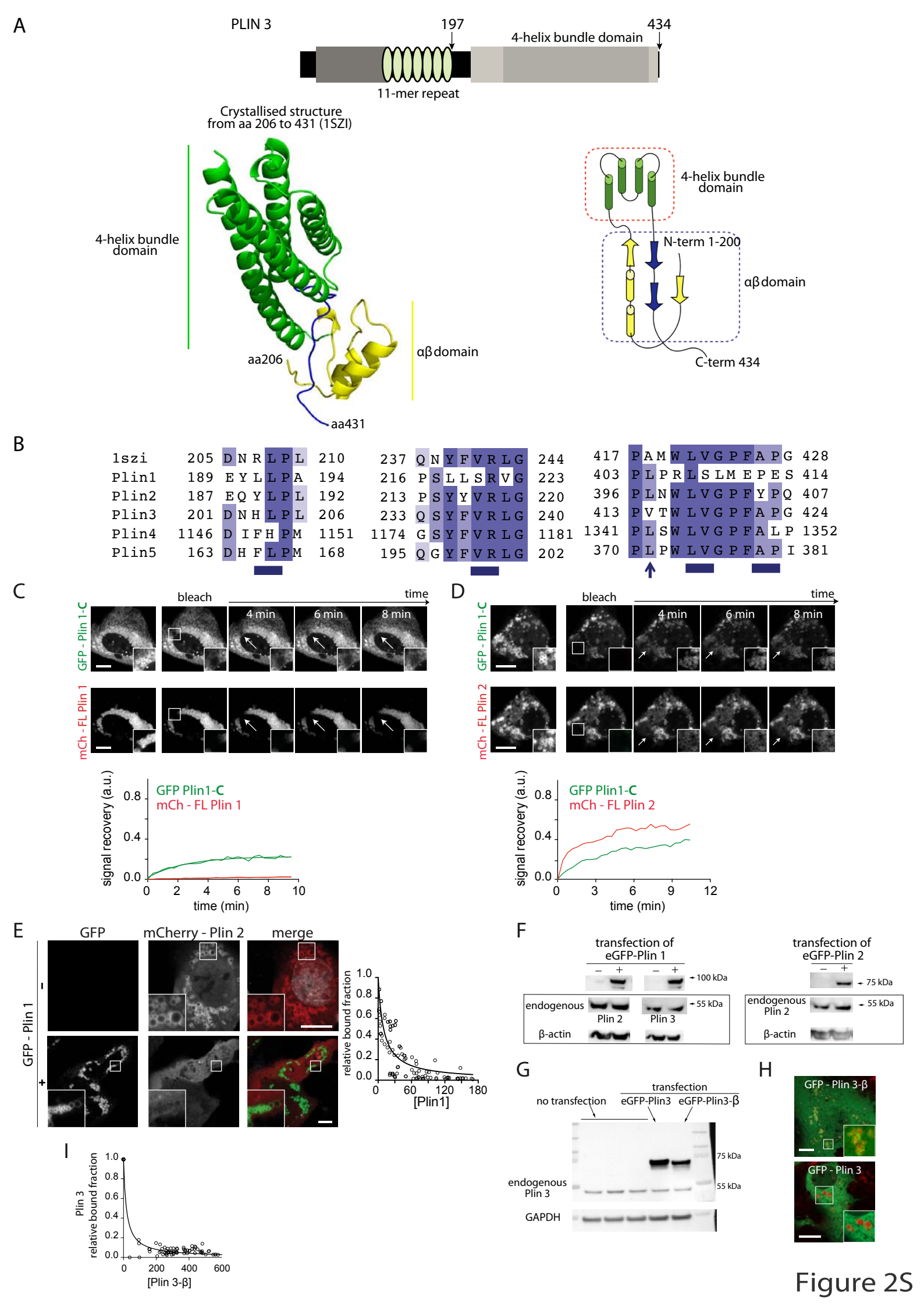
A
PLIN 3
197
434
4-helix bundle domain
11-mer repeat
Crystallised structure
from aa 206 to 431 (1SZI)
4-helix bundle
domain
aa206
αβ domain
aa431
4-helix bundle
domain
N-term 1-200
αβ domain
C-term 434
B
1szi 205 D N R L P L 210 237 Q N Y F V R L G 244 417 P A M W L V G P F A P G 428
Plin1 189 E Y L L P A 194 216 P S L L S R V G 223 403 P L P R L S L M E P E S 414
Plin2 187 E Q Y L P L 192 213 P S Y Y V R L G 220 396 P L N W L V G P F Y P Q 407
Plin3 201 D N H L P L 206 233 Q S Y F V R L G 240 413 P V T W L V G P F A P G 424
Plin4 1146 D I F H P M 1151 1174 G S Y F V R L G 1181 1341 P L S W L V G P F A L P 1352
Plin5 163 D H F L P M 168 195 Q G Y F V R L G 202 370 P L P W L V G P F A P I 381
C
bleach
time
4 min
6 min
8 min
GFP - Plin 1-C
mCh - FL Plin 1
signal recovery (a.u.)
GFP Plin1-C
mCh - FL Plin 1
time (min)
D
bleach
time
4 min
6 min
8 min
GFP - Plin 1-C
mCh - FL Plin 2
signal recovery (a.u.)
GFP Plin1-C
mCh - FL Plin 2
time (min)
E
GFP
mCherry - Plin 2
merge
GFP - Plin 1
relative bound fraction
[Plin1]
F
transfection of
eGFP-Plin 1
transfection of
eGFP-Plin 2
100 kDa
75 kDa
endogenous
Plin 2
Plin 3
55 kDa
β-actin
G
no transfection
transfection
eGFP-Plin3
eGFP-Plin3-β
75 kDa
55 kDa
endogenous
Plin 3
GAPDH
H
GFP - Plin 3-β
GFP - Plin 3
I
Plin 3
relative bound fraction
[Plin 3-β]

Figure 2S

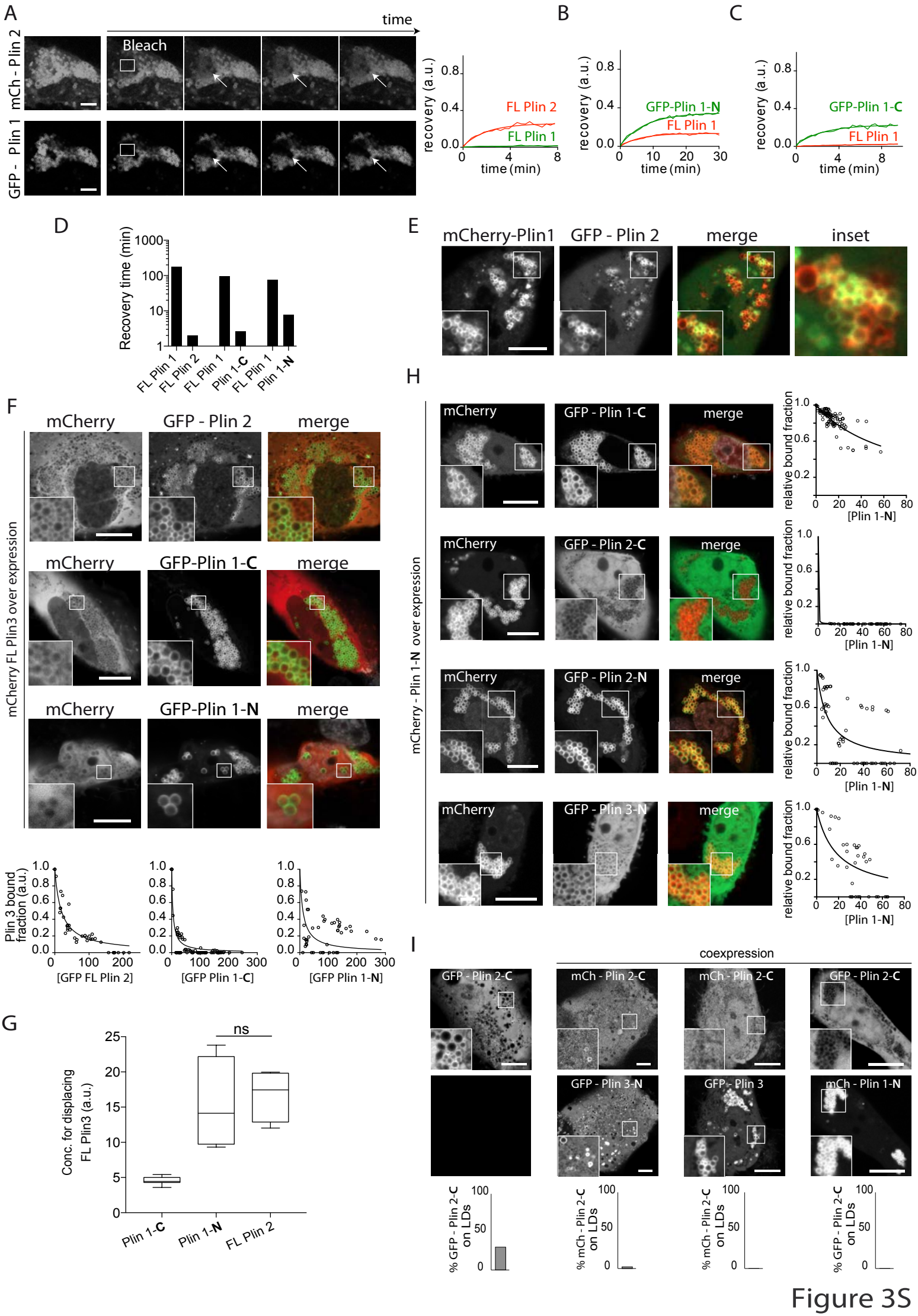
A
time
Bleach
mCh - Plin 2
GFP - Plin 1
B
recovery (a.u.)
FL Plin 2
FL Plin 1
time (min)
C
GFP-Plin 1-N
FL Plin 1
GFP-Plin 1-C
D
Recovery time (min)
FL Plin 1
FL Plin 2
FL Plin 1
Plin 1-C
FL Plin 1
Plin 1-N
E
mCherry-Plin1
GFP - Plin 2
merge
inset
F
mCherry FL Plin3 over expression
mCherry
GFP - Plin 2
merge
GFP-Plin 1-C
GFP-Plin 1-N
Plin 3 bound fraction (a.u.)
[GFP FL Plin 2]
[GFP Plin 1-C]
[GFP Plin 1-N]
G
Conc. for displacing FL Plin3 (a.u.)
ns
Plin 1-C
Plin 1-N
FL Plin 2
H
mCherry - Plin 1-N over expression
mCherry
GFP - Plin 1-C
GFP - Plin 2-C
GFP - Plin 2-N
GFP - Plin 3-N
merge
relative bound fraction
[Plin 1-N]
I
coexpression
GFP - Plin 2-C
mCh - Plin 2-C
GFP - Plin 3-N
GFP - Plin 3
mCh - Plin 1-N
% GFP - Plin 2-C on LDs
% mCh - Plin 2-C on LDs

Figure 3S

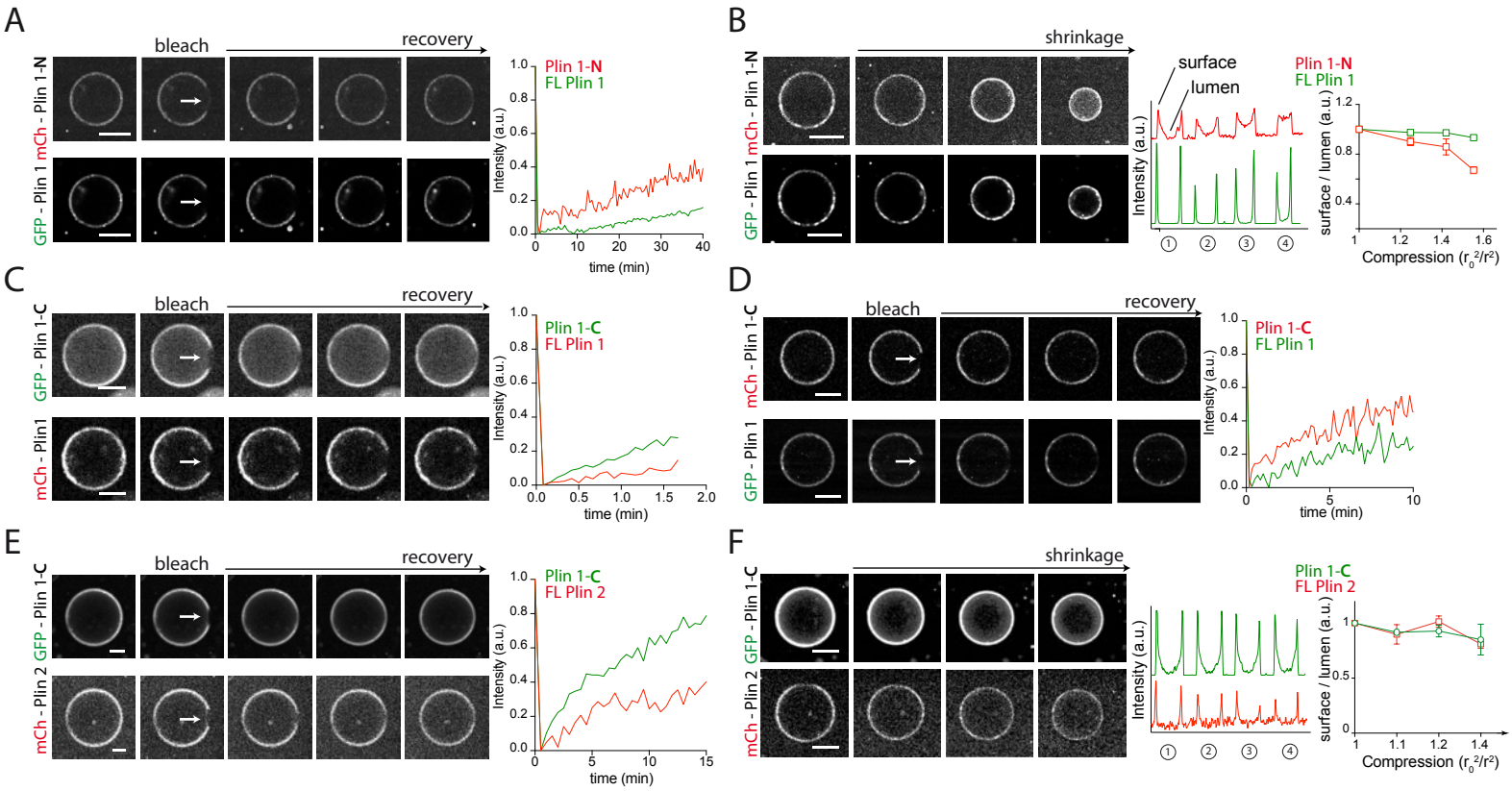
A
bleach
recovery
GFP - Plin 1
mCh - Plin 1-N
Plin 1-N
FL Plin 1
Intensity (a.u.)
time (min)
B
shrinkage
surface
lumen
Plin 1-N
FL Plin 1
Intensity (a.u.)
surface / lumen (a.u.)
Compression (r0²/r²)
C
bleach
recovery
GFP - Plin 1-C
mCh - Plin1
Plin 1-C
FL Plin 1
Intensity (a.u.)
time (min)
D
bleach
recovery
mCh - Plin 1-C
GFP - Plin 1
Plin 1-C
FL Plin 1
Intensity (a.u.)
time (min)
E
bleach
recovery
GFP - Plin 1-C
mCh - Plin 2
Plin 1-C
FL Plin 2
Intensity (a.u.)
time (min)
F
shrinkage
GFP - Plin 1-C
mCh - Plin 2
Plin 1-C
FL Plin 2
Intensity (a.u.)
surface / lumen (a.u.)
Compression (r0²/r²)

Figure 4S

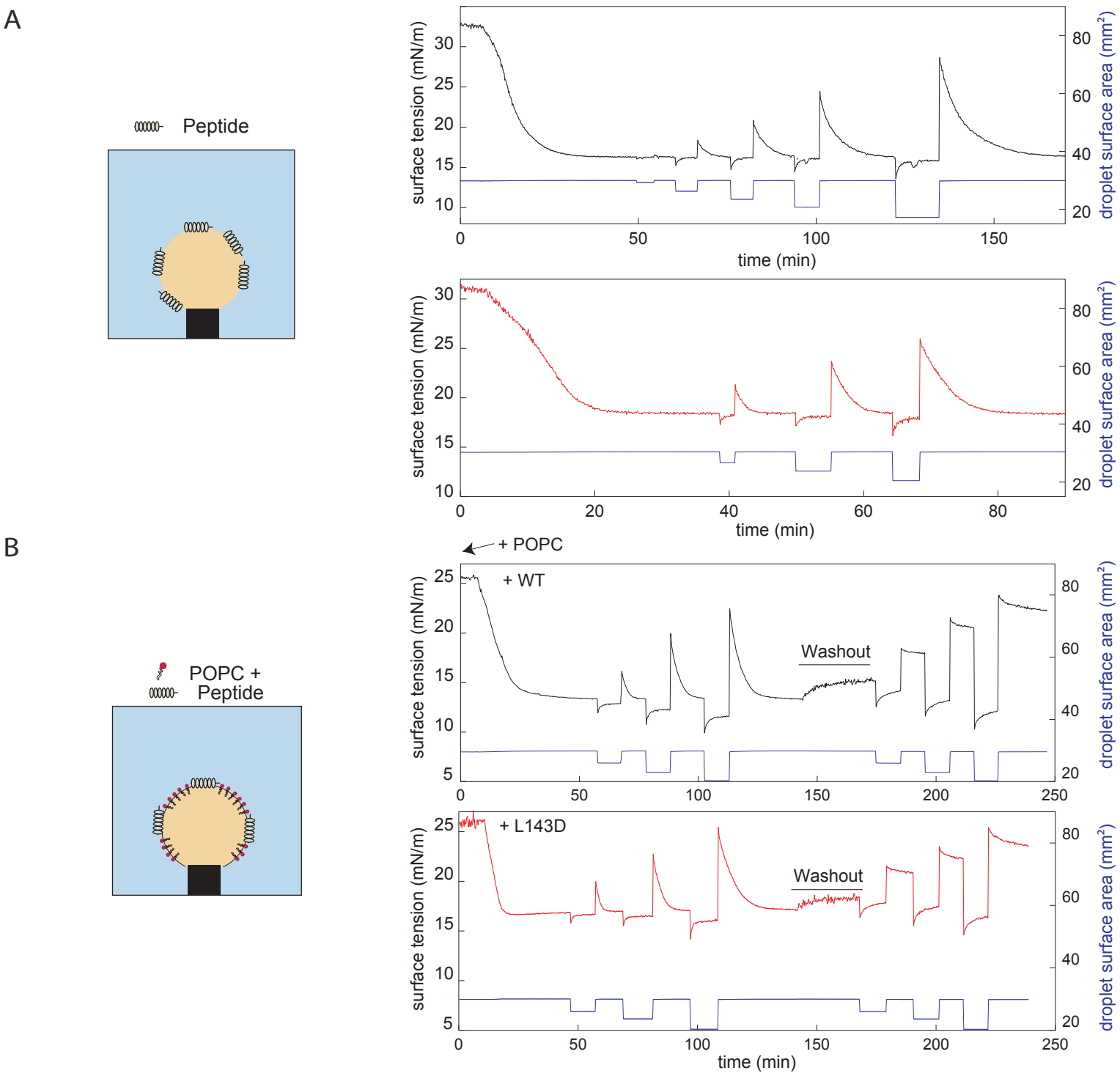
A
Peptide
surface tension (mN/m)
droplet surface area (mm²)
time (min)
B
POPC +
Peptide
+ POPC
+ WT
Washout
+ L143D
Washout
C
+ POPC
+ L143D
+ WT
D
WT
L143D
surface tension increment (mN/m)
surface pressure (mN/m)
POPC + L143D
L143D

Figure 5S